JOINT STUDIES PROGRAMS

As one of the important functions of an inter-university research institute, IMS undertakes joint studies programs for which funds are available to cover research expenses as well as travel and living expenses of individuals. The proposals from domestic scientists are reviewed and controlled by an inter-university committee.

The programs are carried out under one of the following categories:

(1) Joint Studies on Special Projects (a special project of significant relevance to the advancement of molecular science can be carried out by a team of several groups of scientists).
(2) Research Symposia (a symposium on timely topics organized by collaboration between outside and IMS scientists).
(3) Cooperative Research (a research program carried out by outside scientists with collaboration from an IMS scientist).
(4) Use of Facility (a research program carried out by outside scientists at the research facilities of IMS except the UVSOR facility).
(5) Invited Research Project
(6) Joint Studies Programs using beam lines of UVSOR Facility.
(7) Use of Facility Program of the Computer Center (research programs carried out by outside scientists at research facilities in Computer Center).

In the fiscal year 2001, the numbers of joint studies programs accepted for the categories (1)–(7) were 5, 6, 112, 58, 3, 163, and 128, respectively.

(1) Special Projects

A. Studies on Excited State Dynamics by Time-Resolved Photoelectron Imaging

SUZUKI, Toshinori; DE LANGE, Cornelis[1]; TAKATSUKA, Kazuo[2]; MCKOY, Vincent[3]
([1]Univ. Amsterdam; [2]Univ. Tokyo; [3]Caltech)

One of the dreams for molecular scientists is to observe chemical reactions in real time. As electrons moves much faster than nuclei in a molecule, chemical reactions are governed by electronic motions (Born-Oppenheimer approximation). Real-time observation of (non-stationary) electronic states of a molecule is the key for understanding reaction mechanism. Note that an electron has a spin angular momentum and the electronic states with different spin multiplicity come into play in reactions. Previous experimental methods based on optical transitions between the bound states were unable to observe both singlet and triplet states simultaneously with the same wavelength. In 1999, IMS research group has developed a novel experimental means, femtosecond photoelectron imaging where a pump pulse initiates a reaction, and a probe pulse knocks out a valence electron to form a scattering distribution of photoelectrons. The distributions are visualized by two-dimensional position sensitive detection of electrons. The distribution reflects the shape of molecular orbital and nuclear motions that rapidly change during the course of reactions. Since photoionization is allowed from any electronic state, the method probes all the electronic states involved in the reaction. Independently with this experimental research, Tokyo-Caltech research group has been developing a theory for pump-probe photoelectron spectroscopy, in particular photoelectron energy and angular distributions, for exploring non-adiabatic dynamics. This special research program for one and half years was launched to stimulate discussions between experimental and theoretical groups at the frontier.

The laser system is a standard one consisting of an oscillator, an amplifier, and optical parametric amplifiers (OPAs). The output from the oscillator, 80 MHz, 300 mW is introduced into a hybrid chirped pulse amplifier pumped by a Nd:YLF laser. The amplified pulse is a 1 kHz pulse train of ~ 2.5 mJpulse^{-1} light centered at ~ 800 nm with a band width of 13 nm. This amplified light is split into two equal intensity beams to pump two OPAs. Each OPA system has a computer controlled motor drive that adjusts the angles of crystals and a grating to maximize the OPA efficiency at each wavelength. Depending on the experiment, the second, the third, and the fourth harmonics of Ti:sapphire fundamental are also used. The cross-correlation of the pump and probe beams is typically 150–200 fs. The probe beam is optically delayed with respect to the pump beam using a hollow corner cube on a computer-controlled delay stage. The pump and probe laser beams are crossed with a molecular beam in the static electric field in the velocity mapping mode. A pump laser excites molecules in the beam to an electronically excited state, then a probe pulse ionizes the ensemble of molecules. The generated photoelectrons are accelerated parallel to the molecular beam and projected onto a position sensitive imaging detector. The detector consists of a 40 mm diameter dual MCP backed by a phosphor screen. Light from the phosphor is coupled out of the vacuum chamber by means of a fiber bundle where it was recorded by a CCD camera with 512 × 512 pixels. The field-free region of the electron flight path was shielded with a μ-metal tube against stray magnetic fields.

The $S_1(^1B_{3u})$ state of pyrazine has been the best-known example of an intermediate case in molecular radiationless transition theory. Coherent excitation of an intermediate case molecule exhibits a bi-exponential fluorescence decay, where the fast decay is due to the ultrafast dephasing of the optically prepared singlet state

into a mixed singlet-triplet state and the slow decay is the depopulation of this mixed state. This classic problem was revisited by femtosecond TRPEI to shed light on the dark triplet manifold. Figure 1 shows a series of photoelectron images observed by (1+1') REMPI using 324 nm pump and 200 nm probe light at different time delays. These correspond to the 2D sections of the 3D photoelectron scattering distributions: pyrazine molecules are located in the middle of each image, and outgoing photoelectrons are visualized at the point proportional to their scattering velocity vectors. The images observed at short time delays consist of a number of sharp rings. This structure disappears with a lifetime of 110 ps. Correspondingly, a low energy electron signal due to ionization from the triplet manifold grows in the inner part of the image: the triplet levels isoenergetic with the initially photoexcited singlet 0^0 level have large vibrational energies, 4055 cm^{-1}, and the Franck-Condon overlap favors ionization to highly vibrationally excited states in the cation. The sharp rings are transitions to overtone and combination levels of totally symmetric vibrational modes in the cation, and their intensity distribution follows the Franck-Condon factors between the S_1 0^0 level and the cation. The pump and probe polarization directions are parallel to each other in the vertical direction in the figure. The angular anisotropy does exists, yet is rather weak ($\beta \sim 0.3$), reflecting the complex spatial structure of a π^* valence orbital from which an electron is ejected by the probe light. As a conventional way of presentation, the PEDs were extracted from these images by integrating the angular part of the 2D photoelectron scattering distributions, as shown in Figure 2. All the spectra cross at the same energy (isosbestic point), indicating that the spectra consist of two components in dynamic equilibrium. The ionization from the triplet manifold peaks at zero kinetic energy indicating that 200 nm is not a sufficiently short wavelength to ionize the entire vibrational wave-packet in the triplet manifold, making the sensitivity of the experiment to the triplet character relatively less than that for the singlet. Similarly, we have excited pyrazine to various vibronic levels in S_1 ($E_{vib} < 2000$ cm^{-1}) and observed the photoelectron images. In all cases, the singlet signal decayed without changing its structure, meaning that IVR in the S_1 manifold does not occur prior to electronic dephasing due to the lack of sufficient vibrational state density. The same result has been obtained for deuterated pyrazine.

In addition to the electronic and vibrational dynamics, coherent excitation of the P($\Delta J = -1$), Q(0), and R(+1) branch lines creates a superposition of molecular rotational eigenstates, *i.e.* a rotational wave-packet. The constructive and destructive interferences between different *J* components create a time-dependent molecular axis alignment that revives with characteristic time periods determined by rotational constants. Figure 4 shows the rotational revival feature observed for pyrazine S_1 and T_1 states after coherent excitation.

For further detailed examination of rotational wave-packet and its possible use for the study of stereodynamics of molecules, we explored (1+1') and (2+1') REMPI of NO via the $A(^2\Sigma^+)$ 3s Rydberg state. Figure 3 shows the anisotropy parameters of the time-dependent PAD. The rotational temperature in the beam was estimated to be about 20 K, so the NO molecules were populated in the lowest few rotational levels in $^2\Pi_{1/2}$. Since the geometry of a Rydberg state is almost the same as that of a cation, the Franck-Condon propensity upon ionization is $\Delta v = 0$. The photoelectron energy distribution was essentially a single Gaussian function with a width determined by the energy resolution of TRPEI. Although variations of the anisotropy parameters against the time delay were only within 0.1, they were well reproducible and in excellent agreement with the expected time dependence of molecular axis alignment parameter. We have approximated the photoelectron outgoing wave from NO with p and f waves, and determined their transition dipole and phase shifts by analyzing time-dependent photoelectron angular distributions. This is the first report of photoelectorn angular distribution in the molecular frame determined by using a rotational wave packet. The result was compared with theoretical prediction by Professor McKoy and co-workers.

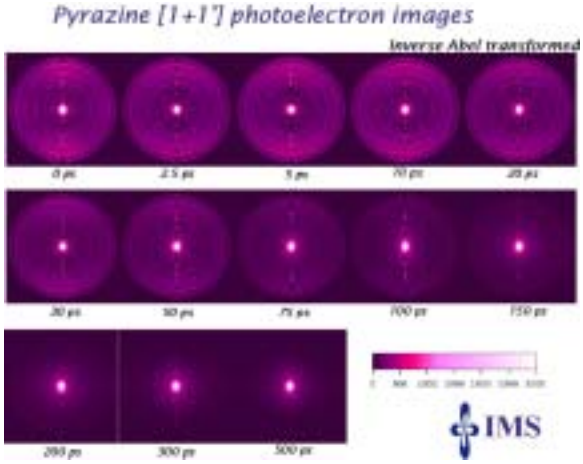

Figure 1. Time-resolved photoelectron images in (1+1') REMPI of pyrazine *via* S_1 0^0 level by pump at 324 nm and probe at 197 nm. The images are inverse Abel transforms of the raw data. The pump and probe laser polarization directions are vertical in the figure.

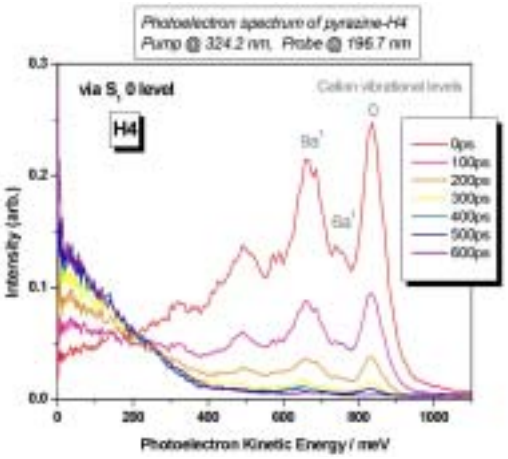

Figure 2. Photoelectron kinetic energy distribution extracted from the images shown in Figure 1.

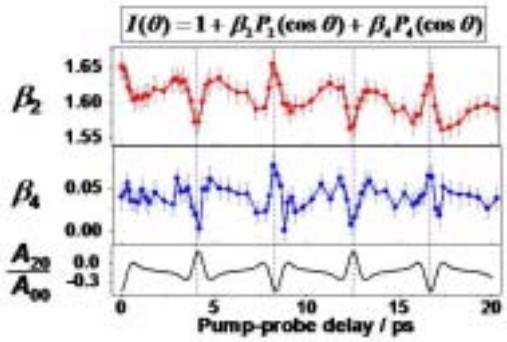

Figure 3. Time-dependent photoelectron anisotropy parameters determined for (1+1') REMPI of NO *via* A ($^2\Sigma^+$) state.

B. Ultrafast Time-Resolved Study on Photochromic Reactions in the Isolated State and Condensed Phase

SEKIYA, Hiroshi[1]; IRIE, Masahiro[1]; SAKURAGI, Hirochika[2]; OKABE, Chie[1]; TANAKA, Nobuyuki[1]; NAKABAYASHI, Takakazu; NISHI, Nobuyuki
([1]Kyushu Univ.; [2]Univ. Tsukuba)

Organic photochromic molecules have been of considerable interests in its potential for the applications to optical memory and light switches. Various types of organic photochromic molecules have been studied. Spiropyran derivatives[1),2)] and azobenzene derivatives[3),4)] are thermally unstable and return to the initial isomers in the dark. In contrast, furylfulgide derivatives[5),6)] and diarylethene derivatives[7),8)] are thermally irreversible photochromic molecules. Among these molecules diarylethene derivatives are the most promising material for applications to optical devices because of their excellent thermal stability, rapid response, and high sensitivity.[7),8)]

A lot of reports have been presented on the photochromic reactions of diarylethene derivatives, and some studies are concentrated on the quantum yields in the cyclization and cycloreversion reactions. The quantum yield must strongly depend on the potential energy surfaces (PES) on which reaction proceeds. However, PES's of diarylethene derivatives have not been well understood. Thus, in this project, we have introduced spectroscopic techniques, which have not been used to investigate photochromic reactions of diarylethene derivatives so far. FT-Raman spectroscopy has been successfully applied to distinguish the open-ring and closed-ring isomers of 1,2-bis(3-methyl-2-thienyl)perfluorocyclopentene (BMTF) in solution (Scheme 1).[9)] Picosecond time-resolved Raman spectroscopy has been used to investigate structural changes of the molecule in the photochromic reaction process.[10)] Electronic spectroscopy is applied to explore the excited-state potential of the open-ring isomer of BMTF in the isolated state.[11)] Now, we are measuring the rates for photochromic reactions of the diarylethenes by time-resolved femtosecond spectroscopy under isolated jet-cooled conditions. We will report on picosecond time-resolved study of diarylethene derivatives in solution and femtosecond time-resolved study of *N*-salicylideneaniline (SA) in the isolated state. Photochromic reaction of SA is originated from excited-state intramolecular proton transfer.

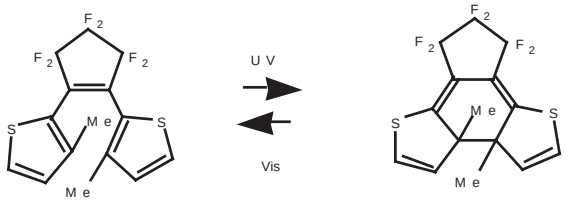

Scheme 1.

B-1 FT-Raman Spectrum of BMTF

Photochromic reaction of BMTF has been studied by FT-Raman spectroscopy.[9)] The Raman bands in the 1400–1600 cm^{-1} region of the open-ring isomer of BMTF are clearly distinguished from those of the closed-ring isomer. The vibrational assignment has been made by measuring the polarized Raman spectrum and density functional theory calculations at the B3LYP/6-31G** level. Two anti-parallel and four parallel conformers are obtained for the open-ring isomer. Among these conformers only the most stable anti-parallel conformer may undergo the cyclization. The FT-Raman spectroscopic study suggests that time-resolved Raman spectroscopy is a promising method to investigate structural change of the molecule during the reaction process.

B-2 Picosecond Time-Resolved Study of Cyclization Reaction of DMTF

The cyclization reaction of 1,2-bis(2,5-dimethyl-3-thienyl)perfluorocyclopentene (DMTF) was investigated by picosecond time-resolved Raman spectroscopy. The UV pulse at 310 nm was used to excite the open-ring isomer, and the visible pulse at 568 nm was used to detect the resonance Raman spectra of the generated closed-ring isomer in the S_0 state. The time-resolved Raman spectra of DMTF in 1-buthanol are shown in Figure 1A. Immediately after the photoexcitation, two Raman bands at 1551 and 1592 cm^{-1} were observed. They are attributable to the closed-ring isomer of DMTF in the electronic ground state (S_0). Figure 1B shows the time-developments of the Raman intensity at 1551 cm^{-1} exhibiting the experimentally limited rise (< 4 ps). This result indicates that the cyclization reaction of BMTF occurs within 4 ps.[10)]

The time-dependence of the peak position of the band at 1551 cm^{-1} is shown in Figure 1C. With increasing the delay time between the pump and probe pulses, its peak position shifts to a higher wavenumber and its bandwidth becomes narrow. This change is associated with intermolecular vibrational relaxation of the closed-ring isomer of the vibrational excited state.

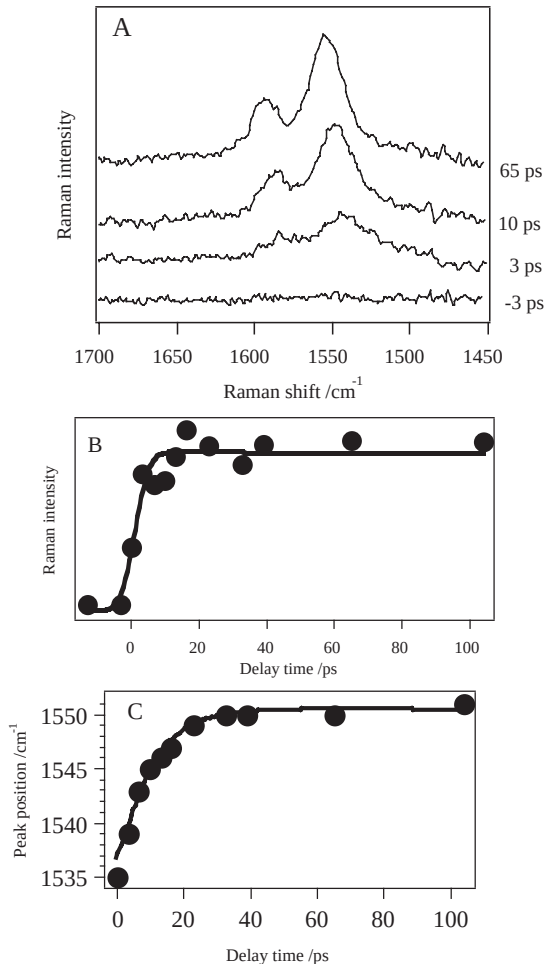

Figure 1. Picoseond time-reosolved Raman spectra of DMTF in 1-butanol (**A**), Plots of the Raman intensity of DMTF at 1551 cm^{-1} against the delay time (**B**), and temporal change of the frequency of the band around 1550 cm^{-1} of BMTF against the delay time (**C**).

B-3 Picoseond Time-Resolved Study of Cycloreversion Reaction of BMPTF

The cycloreversion reaction has been studied with 2-bis(3-methyl-5-phenyl-2-thienyl)perfluorocyclopentene (BMPTF) by using picosecond time-resolved anti-Stokes Raman spectroscopy. The pump and probe wavelengths were 480 and 395 nm, respectively. These wavelengths correspond to the absorption regions of the closed-ring and open-ring forms of BMPTF, respectively.

Figure 1 shows the anti-Stokes Raman spectra of BMPTF at 2 and 8 ps. The intensity scale is normalized for the peak intensity at 1610 cm^{-1}, which is assigned to the C=C stretching mode of the cyclopentene moiety. The change in the relative intensity of the anti-Stokes Raman bands was observed. It has been shown that a part of excess energy generated via the cylcoreversion reaction is localized on the C=C stretching mode of the cyclopentene moiety. This means that the C=C stretching mode is one of the accepting modes in the cycloreversion process.

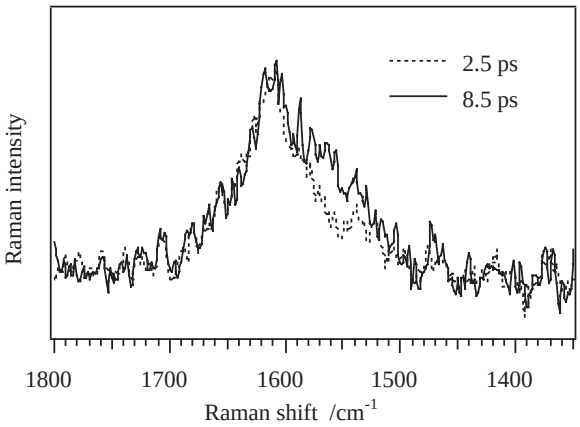

Figure 1. Picosecond time-resolved anti-Stokes Raman spectra of BMPTF in acetonitrile. The intensity of each spectrum is normalized by reference to the intensity of the band at 1610 cm^{-1}.

B-4 Femtosecond Time-Resolved Study of *N*-Salicylideneaniline in the Isolated State

The excitation of the enol-form of *N*-salicylideneaniline (SA) produces the keto-form through excited-state intramolecular proton transfer (Scheme 1). The laser induced fluorescence excitation and dispersed fluorescence spectra of jet-cooled SA have been observed in a supersonic free jet for the first time. The spectrum shows a very broad feature with no vibronic structure in the 24800–29000 cm^{-1} region except for a broad peak at 28200 cm^{-1}. The broad feature of the spectrum has been ascribed to the homogeneous broadening of vibronic bands due to very fast internal conversion from the $^1\pi\pi^*$ to $^1n\pi^*$ state which is located below the $^1\pi\pi^*$ state as well as to the excited-state intramolecular proton transfer reaction.[12] No resonance emission has been detected following the excitation of the $^1\pi\pi^*$ state of the enol form, while anomaly Stokes-shifted fluorescence was observed at 15000–20500 cm^{-1}. The dispersed fluorescence spectra show two broad maxima separated by 700–1000 cm^{-1}, suggesting that two keto tautomers are produced via the excited-state intramolecular proton transfer reaction. The existence of the corresponding two cis-keto tautomers with similar energies has been suggested by density functional theory calculations at the B3LYP/6-31G** level and ab initio calculations at the HF/6-31G** level.

In order to examine the above conclusion obtained from the electronic spectroscopy of jet-cooled SA the pump and probe technique with the detection of ion signal generated by multi-photon ionization has been applied to determine the decay rate of the excited state of the enol-form. Figure 1 shows a typical decay curve. The decay curve is fitted by bi-exponential function with two decay rate constants: fast decay is less than 250 fs and slow decay is 1.7 ps. The fast component is ascribed to the decay of initially photoexcited $^1\pi\pi^*$ state due to excited-state proton transfer and fast internal conversion to the $^1n\pi^*$ state, while the slow component to the decay of the $^1n\pi^*$ state. These results are in good agreement with the conclusion derived from the electronic spectroscopy.

We have observed the fluorescence and dispersed fluorescence spectra of jet-cooled BMTF. It has been

shown that the initially photoexcited electronic state is not the S_1 state but the S_2 state and fast internal conversion occurs from the S_2 state.[11] The experiment of ultrafast time-resolved spectroscopy is in progress to investigate the fast internal conversion process and to determine the photochromic reaction rates of diarylethene derivatives. A very close similarity exists in the excited state potential of SA and diarylethene derivatives. Femtosecond time-resolved study may provide consistent results with those obtained from the fluorescence spectroscopy.

References

1) M. Hirano, A. Miyashita and H. Nohira, *Chem. Lett.* 209 (1991).
2) O. Pieroni, A. Fissi, N. Angelini and F. Lenci, *Acc. Chem. Res.* **34**, 9 (2001).
3) E. Sackmann, *J. Am. Chem. Soc.* **93**, 7088 (1971).
4) H. Rav and E. Luddecke, *J. Am. Chem. Soc.* **104**, 1616 (1982).
5) P. J. Darcy, H. G. Heller, P. J. Stryldom and J. Whittall, *J. Chem. Soc. Perkin I* 202 (1981).
6) Y. Yokoyama, *Chem. Rev.* **100**, 1717 (200).
7) M. Irie and M. Mohri, *J. Org. Chem.* **53**, 803 (1988).
8) M. Irie, *Chem. Rev.* **100**, 1685 (2000).
9) C. Okabe, N. Tanaka, T. Fukaminato, T. Kawai, M. Irie, Y. Nibu, H. Shimada, A. Goldberg, S. Nakamura and H. Sekiya, *Chem. Phys. Lett.* **357**,113 (2002).
10) C. Okabe, T. Nakabayashi, N. Nishi, T. Fukaminato, T. Kawai, M. Irie and H. Sekiya, The First Symposium on "Understanding of Nonequilibrium-Nonstationary Characteristics Specific to Chemical-Reacting Phenomena—Reconsideration of Statistical Theory from the Viewpoint of Modern Chemistry," (March 8–10, Okazaki).
11) N. Tanaka, C. Okabe, K. Sakota, T. Fukaminato, T. Kawai, M. Irie, A. Goldberg, S. Nakamura and H. Sekiya, *J. Mol. Struct.* **616**, 113 (2002).
12) N. Otsubo, C. Okabe, H. Mori, K. Sakota, K. Amimoto, T. Kawato and H. Sekiya, *J. Photochem. Photobiol. A (Chemistry)*, Special Issue on Photo-induced Proton Transfer, in press.

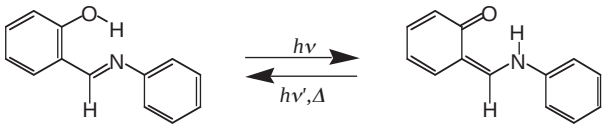

Scheme 1.

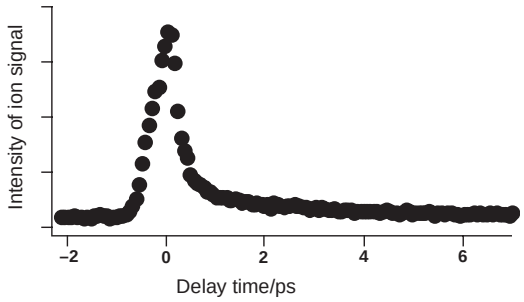

Figure 1. Decay curve obtained by exciting the enol tautomer of *N*-salycilideneaniline in the isolated jet-cooled conditions. Ion signal was detected as a function of the delay time of the ionization pulse.

C. Development of Effective Generalized-Ensemble Algorithms for Complex Systems with Many Degrees of Freedom

OKAMOTO, Yuko; SUGITA, Yuji; NAGASIMA, Takehiro; MITSUTAKE, Ayori[1]; NAKAZAWA, Takashi[2]; YUMINAGA, Hiroko[2]; BERG, Bernd A.[3]
([1]Keio Univ.; [2]Nara Women's Univ.; [3]Florida State Univ.)

Complex systems with many degrees of freedom such as spin glasses and biopolymers have a huge number of local minima in potential energy. Conventional constant-temperature simulations based on canonical ensemble will thus tend to get trapped in states of energy local minima. Generalized-ensemble algorithms, which are based on artificial non-Boltzmann weight factors, alleviate this multiple-minima problem by performing random walks in potential energy space, allowing the simulation to explore a much wider range of the configurational space than by conventional methods. The advantage of generalized-ensemble algorithms lies in the fact that from only one simulation run, one can obtain not only the global-minimum state in potential energy but also various thermodynamic quantities as a function of temperature. Multicanonical algorithm, simulated tempering, and replica-exchange method are well-known examples of generalized-ensemble algorithms and have been widely used in simulations of spin systems and protein systems. However, as the system becomes complex, the application of these algorithms faces technical difficulties. In the first two methods, the determination of the non-Boltzmann weight factors becomes very time-consuming. In the third method, on the other hand, the weight factor determination is trivial, but much more simulation time is required for the production run than in the first two methods. Recently, we have developed new effective generalized-ensemble algorithms that combine the merits of these three generalized-ensemble algorithms (for a recent review, see A. Mitsutake, Y. Sugita and Y. Okamoto, *Biopolymers (Peptide Science)* **60**, 96 (2001)). The purpose of the present project is to further test the effectiveness of these new methods by performing simulations of spin systems and protein systems and to develop even more powerful generalized-ensemble algorithms.

C-1 Generalized-Ensemble Simulations of Spin Systems and Protein Systems

[*Comput. Phys. Commun.* **146**, 69 (2002)]

We test the effectiveness of the recently proposed generalized-ensemble algorithms that combine the merits of multicanonical algorithm and replica-exchange method, namely, replica-exchange multicanonical algorithm (REMUCA) and multicanonical replica-exchange method (MUCAREM). A spin system and protein systems were used for the test. For the former, two-dimensional 10-state Potts model was simulated. For the latter, various short peptide systems both in gas phase and in aqueous solution were simulated. REMUCA and MUCAREM present new methods for the multicanonical weight factor determination. It was shown for the

Potts model case that these methods are at least as powerful as the most effective method that was known previously.

D. Study on the Magnetization of the Supra-Molecule Built by Fullerenes

KATO, Tatsuhisa; TOYAMA, Namiki; TASHIRO, Kentaro[1]; AKASAKA, Takeshi[2] ; AIDA, Takuzo[1]; YAMAUCHI, Seigo[3]; DINSE, Klaus-Peter[4]
([1]Univ. Tokyo; [2]Univ. Tsukuba; [3]Tohoku Univ.; [4]Darmstadt Univ. Tech.)

An endohedral metallofullerene is the building-block molecule for the nano-scaled structure with ferromagnetism. On the other hand an association of a porphyrin with C_{60} is well known, and an inclusion through π-electron donor-acceptor interaction is highly interesting in view of the construction of a supramolecule. Moreover the system composed of a metalloporphyrin with a metallofullerene leads to other attention of the parallel alignment of spins via spin exchange interaction, which is the key issue of the ferromagnetism. Tokyo group synthesized a face-to-face cyclic dimer of metalloporphyrin and reported that a cyclic dimer of zinc-porphyrin (Zn-PD) forms an inclusion complex with C_{60} (Zn-PD+C_{60}), of which the association constant K_{assoc} of 6.7×10^5 M^{-1} is much higher than those of organic media reported to date. If a copper-porphyrin dimer (Cu-PD) is used as a host molecule, there are two radical sites in the system, and a question arises as to whether the two radical sites couple or not. When a spin-labeled fullerene of La@C_{82} is introduced between the two radical sites of Cu-PD, the assignment of the resultant spin state of the inclusion complex (Cu-PD+La@C_{82}) comes into the final question.

E. Magnetic Anisotropy and Magnetic Viscosity of Chiral Molecule-Based Magnets

INOUE, Katsuya; HOSOKOSHI, Yuko; BARANOV, Nikolai[1]; NAKAMURA, Nobuo[2]; ISHIZUKA, Keita[2]; SAKAGUCHI, Takahiro[2]
([1]IMS and Ural State Univ.; [2]Housei Univ.)

Magnetic anisotropy is an important characteristic feature of magnets. Molecule-based magnets can control the dimensionality of magnetic structure of spins. These magnets show clear magnetic anisotropy and easy to analyze by the magnetic single crystal measurements. Recently, we designed and synthesized many chiral molecule-based magnets. In the chiral magnets, the magnetic moments located in asymmetrical position and the magnetic dipole fields are also asymmetric. The magnetic anisotropy of these materials is great interesting. In the program, we planned to make new low dimensional chiral magnets and study for magnetic anisotropy and magnetic viscosity of these magnets.

E-1 Synthesis and Structural Studies of New One-Dimensional Chiral Molecule-Based Magnets

In 1999, we have already made a chiral metamagnet with a T_N = 5.5 K (**1**•Mn(hfac)$_2$) and a ferrimagnet with a T_C = 4.5 K (**2**•Mn(hfac)$_2$). These magnets are small brown and blue single crystals, respectively. The sizes of these crystals are less than ca. 0.5 mm, this size crystal is too small for single crystal magnetic measurements. The crystallizability of materials depends on the solubility and/or molecular shapes. Usually, planer molecules have good crystallizability than the bulky molecules. Then we design new organic radicals to make large single crystals.

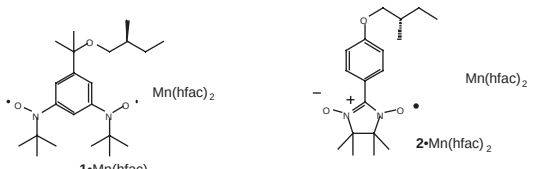

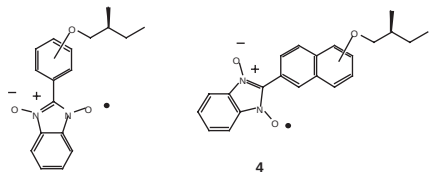

The synthetic route of the new chiral bidendate monoradicals radical **3** is illustrated in Figure 1. *p*- and *m*- isomer were obtained as green solid and green oil, respectively. Complexation with bishexafluoroacetylacetonate manganese are now in progress.

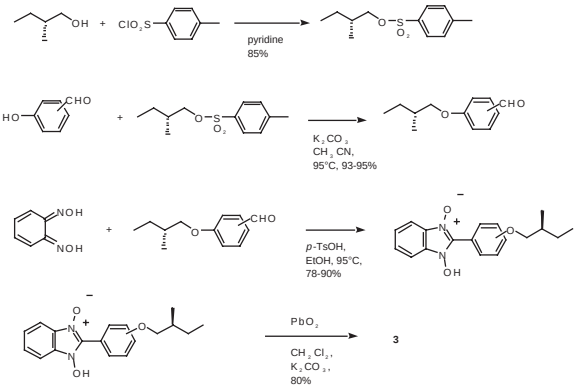

Figure 1.

F. Thermal and Optical Switching of Spin-Crossover Compounds

HAYAMI, Shinya[1]; HOSOKOSHI, Yuko; INOUE, Katsuya; SATO, Osamu[2]; MAEDA, Yonezo[1]
([1]Kyushu Univ.; [2]KAST)

The design of molecules, which can be utilized for information processing and information storage, is one of the main challenges in molecular materials science. The molecules for such purpose must exhibit bistability, which may be defined as the property of a molecular

system being able to exist in two different electronic states in a certain range of external perturbation. Typical example of molecular species exhibiting such molecular bistability is spin crossover complexes. Since the discovery of the first spin-crossover complex, a variety of d^n (n = 4–7) transition metal compounds exhibiting bistability between high-spin (HS) and low-spin (LS) states have been reported. Usually, the spin transition phenomena can be induced by a variation of temperature or of pressure. On the other hand, Decurtine et al. show that the spin transition can be induced by illumination in 1984. This finding shows that the spin-crossover compounds have potential applications for optical switches and data storage devices. Here we purpose to develop the optical switching molecular devices.

F-1 Photo-Induced Spin Transition for Iron(III) Compounds with π-π Interactions

JUHASZ, Gergely[1]; HAYAMI, Shinya[1]; SATO, Osamu[2]; MAEDA, Yonezo[1]
([1]Kyushu Univ.; [2]KAST)

[*Chem. Phys. Lett.* in press]

The magnetic susceptibilities of the spin-crossover compound $[Fe(pap)_2]PF_6$·MeOH (**1**) have been measured and compared with that of the previously reported compound $[Fe(pap)_2]ClO_4$·H_2O (**2**). Compound **1** is a spin-crossover compound with spin transition temperature $T_{1/2}$ = 288 K, and does not show a hysteresis loop around the spin transition temperature, in contrast with compound **2**. Magnetic susceptibilities measured after illumination prove that **1** exhibits the LIESST effect, so does compound **2**. The crystallographic data on the molecular packing show the presence of π stacking between the aromatic rings of pap ligands, which appears to be responsible for the LIESST effect.

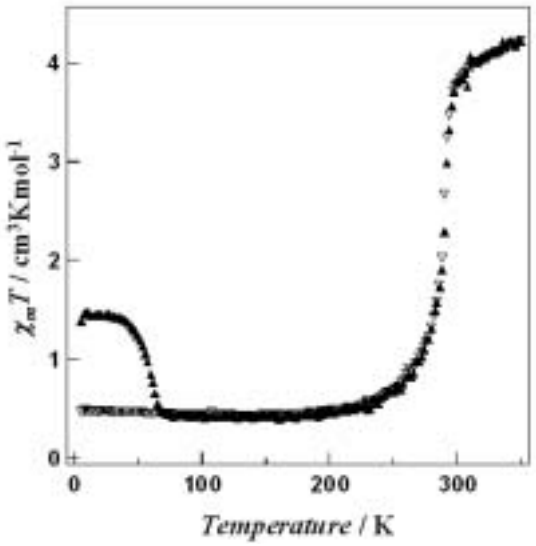

Figure 1. Photomagnetic behavior: $\chi_m T$ of $[Fe(pap)_2]PF_6$·MeOH(**1**) as a function of temperature on cooling (▽), after irradiated at 5 K and warming up (▲).

F-2 Crystal Structure of a Molecular Building Block with π-π Intermolecular Interaction

HAYAMI, Shinya[1]; KAWAMURA, Kazunori[1]; JUHASZ, Gergely[1]; KAWAHARA, Takayoshi[1]; UEHASHI, Keigo[1]; MAEDA, Yonezo[1]
([1]Kyushu Univ.)

[*Mol. Cryst. Liq. Cryst.* **379**, 371 (2002)]

Mononuclear iron(II) compound $[Fe(4tpt)_2(NCS)_2(MeOH)_2]$·MeOH (**1**) (4tpt = 2,4,6-tri(4-pyridyl)-1,3,5-triazine) was synthesized and characterized by X-ray single crystal diffraction, Mössbauer spectra, magnetic susceptibilities, electronic spectra and IR spectra. The crystal structure of **1** was determined. Crystal data for **1**: $C_{42}H_{40}O_4N_{14}S_2Fe_1$, space groupe *P-1*, Z = 2, a = 7.091(1), b = 10.630(2), c = 28.251(7) Å, α = 89.77(1)°, β = 90.072(9)°, γ = 84.45(1)°, V = 2119.5(7) Å^3, $R1$ = 0.069. The compound **1** has two 4tpt ligands, and forms π-π stacking between the 4tpt ligands in the neighboring complexes along the *b* axis. The assembly of the constituent complexes forms 1-D zigzag chains because of the strong π-π stacking between the neighboring complexes. Two methanol molecules are contained in the space between the 1-D zigzag chains.

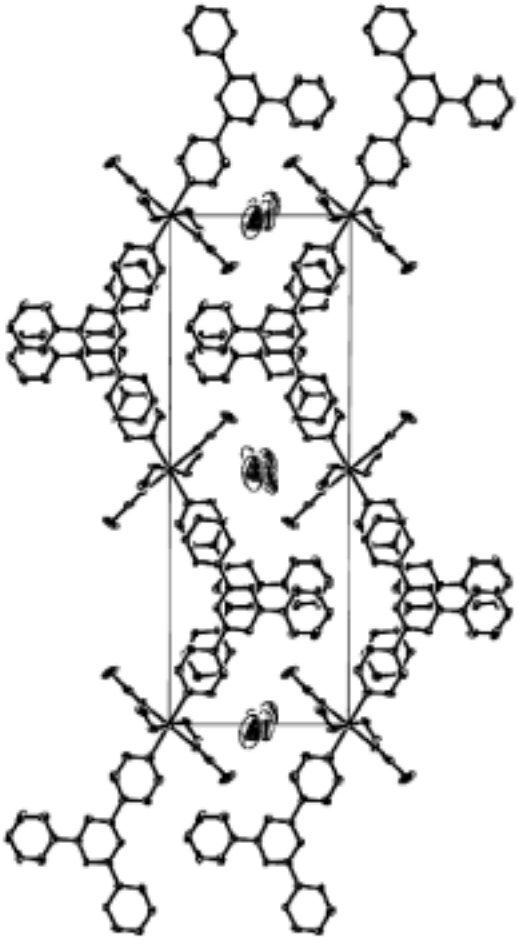

Figure 1. Crystal packing view of $[Fe(4tpt)_2(NCS)_2(MeOH)_2]$·MeOH(**1**) with π-π stacking between complexes.

F-3 Study of Intermolecular Interaction for the Spin-Crossover Iron(II) Compounds

HAYAMI, Shinya[1]; KAWAJIRI, Ryo[1]; JUHASZ, Gergely[1]; KAWAHARA, Takayoshi[1]; SATO, Osamu[2]; MAEDA, Yonezo[1]
([1]Kyushu Univ.; [2]KAST)

[submitted]

In the iron(II) spin-crossover compounds [Fe(PM-iPA)$_2$(NCS)$_2$] (**1**) and [Fe(PM-iPA)$_2$(NCSe)$_2$] (**2**) (PM-iPA = *N*-2'-pyridylmethylene)-isopropylamine)) with ligand having bulky substitute, the thermal spin transition have occurred at $T_{1/2}$ = 267 K and 376 K without thermal hysteresis, respectively. The compounds **1** and **2** could not be observed light-induced excited spin state trapping (LIESST) effect even at 5 K. On the other hand, Létard *et al.* have reported that the iron(II) spin-crossover compounds [Fe(PM-L)$_2$(NCX)$_2$] (L = A, BiA, TeA, PEA and AzA; X = S and Se) with ligands having π system exhibited thermal spin transition, respectively. The iron(II) compounds have exhibited LIESST effect, and the critical LIESST temperature, T_c(LIESST), has been observed. The structure of **1** and **2** are crystallized at *Pnna* and *C2/c* at room temperature, respectively, and structure of low-spin state are also same space group without structural change. The structures of the iron(II) compounds with π system ligands also have been reported in the high-spin state, and the structure in the low-spin state remain if the compounds occurred spin transition. It has been found that the compound **1** and **2** have not form any intermolecular interactions between the complexes, while the compounds with π system ligands form π-π intra- and intermolecular interactions in the ligands. It is thought that the intermolecular interactions play an important role in the trapping a light-induced metastatble state.

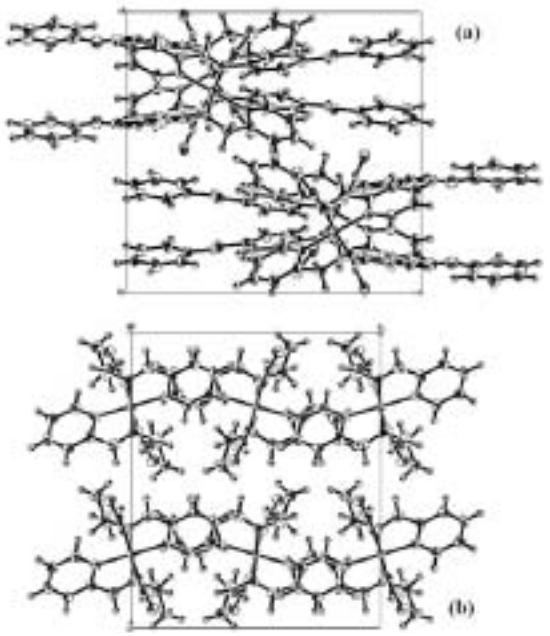

Figure 1. Crystal packings of (a) [Fe(PM-iPA)$_2$(NCS)$_2$](**1**) and (b)[Fe(PM-AzA)$_2$(NCS)$_2$](**3**) in the low-spin state.

F-4 The High-Spin → Low-Spin States Relaxation in Iron(III) Compounds

HAYAMI, Shinya[1]; HOSOKOSHI, Yuko; INOUE, Katsuya; SATO, Osamu[2]; MAEDA, Yonezo[1]
([1]Kyushu Univ.; [2]KAST)

During the past years many studies have been performed on the dynamics of the HS → LS relaxation, especially for iron(II) spin-crossover compounds in solution and at ambient temperatures. Different experimental methods were used to determine the rate constants k_{HL} of the HS → LS relaxation. After the studies of McGarvey and Lawthers, however, pulsed laser excitation has become the most common technique. For iron(II) spin-crossover complexes, HS → LS relaxation rates and activation parameters determined with line sape analysis of Mössbauer spectra in the solid state around room temperature were similar to those in solution. This technique, however, is restricted to systems with transition temperature $T_{1/2}$ around room temperature, because at temperatures where the rate constants k_{HL} fit into the Mössbauer time window of 10^6 $s^{-1} \leq k_{HL} \leq 10^8$ s^{-1}, HS and LS species must be simultaneously present in sufficient concentrations. With the discovery of LIESST and the elucidation of the mechanism of light-induced population of metastable HS states, new possibilities to study HS → LS relaxation in the solid and at low temperatures were opened. Here we show the HS → LS relaxation and the rate constants k_{HL} for iron(III) LIESST complex.

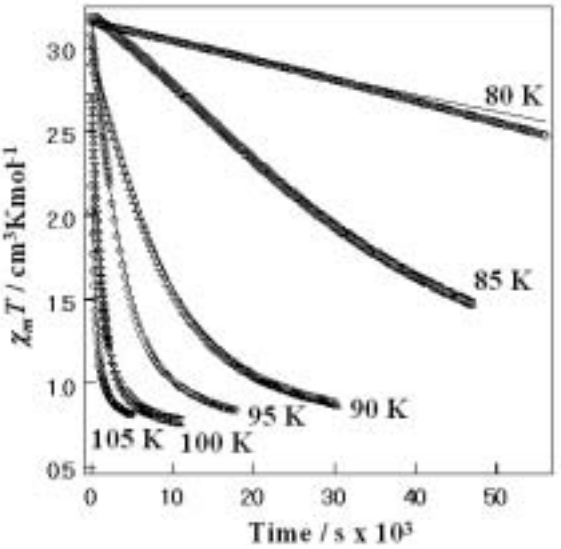

Figure 1. Dependence of $\chi_m T$ on time for the HS → LS transformation in quenched-in [Fe(pap)$_2$]ClO$_4$.

(2) Research Symposia

(from September 2001 to August 2002)

1. New Developments in Molecular Science Research using Scanning Probe Microscopy
   (February 14-15, 2002)
   Chair: **KOMIYAMA, Masaharu**

2. Atomic and Molecular Dynamics on Valence Excitation and Ionization
(February 18-19, 2002)
Chair: **KOUCHI, Noriyuki**

3. Water and Biomolecules Cooperate in Chemistry of Life
(May 15-17, 2002)
Chair: **HIRATA, Fumio**

4. Symposium of Molecular Science
(May 17-18, 2002)
Chair: **KAJIMOTO, Okitsugu**

5. Symposium on Physical Chemistry for Young Researchers of Molecular Science
(June 5, 2002)
Chair: **KATO, Hajime**

6. Current Status and Future Prospect of Dynamics of Photon, Electron and Heavy-particle Collisions
(July 25-26, 2002)
Chair: **TAKAHASHI, Masahiko**

(3) Cooperative Research

This is one of the most important categories that IMS undertakes for conducting its own research of the common interest to both outside and IMS scientists by using the facilities at IMS. During the first half of the fiscal year of 2001 ending on September 30, 99 outside scientists from 47 research groups joined the Cooperative Research programs, and during the second half, 107 outside scientists from 65 research groups joined the programs. The names and affiliations of those collaborations are found in the Research Activities sections in this Review.

(4) Use of Facility

The numbers of projects accepted for the Use-of-Facility program during the first half and the second half of the fiscal year of 2001 amounted to 2 and 5 for the Laser Research Center for Molecular Science, 24 and 27 for the Research Center for Molecular Materials (the Research Center for Molecular-scale Nanoscience from April 1, 2002), and 0 and 0 for Equipment Development Center, respectively.

(5) Invited Research

Under this joint-study program, several scientists were invited from other institutions of help for construction and improvement of instruments in IMS. The total number of the projects in this category was 3 (2 for the first half and 1 for the second half) in the fiscal year of 2001.

(6) Use of UVSOR Projects

In the UVSOR Facility with the 750 MeV electron storage ring, there are twenty beam lines available for synchrotron radiation research (see UVSOR ACTIVITY REPORT 2001). Under the Use of UVSOR Projects, many synchrotron radiation experiments have been carried out by outside scientists on eleven beam lines in close cooperation with the UVSOR staff. The total number of the projects in this category was 163 (82 for the first half and 81 for the second half) in the fiscal year of 2001.

(7) Use of Facility Program of the Computer Center

Computer Center provides three types of research programs for outside scientists: (a) Use-of-Facility Program; (b) Cooperative Research Program; (c) Advanced Research Program. The numbers of projects accepted for each programs during the fiscal year of 2001 were (a) 124 with 499 users, (b) 4 with 6 users (2 projects for the first half and 2 projects for the second half) and (c) 0 with 0 users. Computer time distributed to these projects amounted to 73% of the total annual CPU time.